JOM
https://doi.org/10.1007/s11837-018-3098-3

Effect of Infiltration of Barium Carbonate Nanoparticles on the Electrochemical Performance of $La_{0.6}Sr_{0.4}Co_{0.2}Fe_{0.8}O_{3-\delta}$ Cathodes for Protonic Ceramic Fuel Cells

JUN GAO,[1] YUQING MENG,[1] SHIWOO LEE,[2,3] JIANHUA TONG,[1] and KYLE S. BRINKMAN[1,2,4]

1.—Department of Materials Science and Engineering, Clemson University, Clemson, SC 29634, USA. 2.—U.S. Department of Energy, National Energy Technology Laboratory, 3610 Collins Ferry Rd, PO Box 880, Morgantown, WV 26507-0880, USA. 3.—AECOM, Morgantown, WV 26507, USA. 4.—e-mail: ksbrink@clemson.edu

$BaCO_3$ nanoparticles were infiltrated into a $La_{0.6}Sr_{0.4}Co_{0.2}Fe_{0.8}O_{3-\delta}$ (LSCF) electrode as a synergistic catalyst to enhance the performance of proton conducting solid oxide fuel cells (H-SOFCs). Electrochemical impedance analysis showed that the polarization resistance was dramatically reduced by nearly 75% from 1.123 Ω cm^2 to 0.293 Ω cm^2 at 700°C after infiltration of $BaCO_3$ nanoparticles. The chemical stability between the $BaCO_3$ and LSCF electrode was investigated by running a long-term 300-h test, during which the polarization resistance exhibited only minor degradation (2.22–2.20 Ω cm^2). In addition, single cells with infiltrated LSCF electrode and $BaCe_{0.7}Zr_{0.1}Y_{0.1}Yb_{0.1}O_{3-\delta}$ (BCZYYb) electrolyte yielded a maximum power density of 404 mW cm^{-2} at 700°C, much higher than cells with a bare LSCF electrode (268 mW cm^{-2} at 700°C). $BaCO_3$ demonstrated promising performance enhancements of LSCF electrodes for H-SOFCs and warrants further development.

INTRODUCTION

Solid oxide fuel cells (SOFCs) can efficiently convert chemical energy in fuel into electricity with limited by-products.[1–4] However, their elevated working temperature (800–1000°C) and long-term performance/durability remain as main obstacles limiting practical applications. Proton-conducting SOFCs (H-SOFCs) have attracted increasing interest in recent years due to their lower working temperature (400–700°C) and the lower activation energy for proton transport compared with oxygen ion systems.[5]

For a given electrolyte with a specific thickness, the chemical reaction at the cathode is the main factor determining SOFC performance.[6] To improve the oxygen reduction reaction (ORR) at the cathode, two approaches have been utilized: (1) compositional modifications such as those of Haile and Shao,[7] who pioneered high-performance $Ba_{0.5}Sr_{0.5}Co_{0.8}Fe_{0.2}O_{3-\delta}$ (BSCF) cathodes, and (ii) optimization of the electrode microstructure; For example, synthesis methods such as the phase inversion technique have been employed to produce aligned pores and thereby reduce the diffusion barrier.[8] An additional method which combines compositional and microstructural modification is infiltration to achieve a nanoscale electrode with greater area for catalytic reaction.[9,10]

Significant work has been performed on infiltration of nanoparticles to increase the oxygen catalytic activity at the cathode in oxygen ion SOFCs (O-SOFCs). However, limited work to date has focused on improving the cathode performance of H-SOFCs through infiltration. $La_{0.6}Sr_{0.4}Co_{0.2}Fe_{0.8}O_{3-\delta}$ (LSCF) is a widely used cathode with excellent mixed electronic–ionic conductivity at intermediate temperatures,[11,12] but suffers from low electronic conductivity at low temperatures. Lei[13] reported $PrNi_{0.5}Mn_{0.5}O_3$ and PrO_x as infiltration materials for LSCF electrodes of H-SOFCs, indicating that the hybrid catalyst significantly improved the cathode reaction kinetics and fuel cell performance. Li[14] infiltrated the oxygen ion conductor $Y_{0.25}Bi_{0.75}O_{1.5}$ into a LSCF electrode, resulting in decreased interfacial polarization resistance. He et al.[15] deposited

Published online: 28 August 2018

$Gd_{0.1}Ce_{0.9}O_{1.95}$ nanoparticles into a LSCF electrode, decreasing the polarization resistance from 10.77 Ω cm^2 to 2.47 Ω cm^2 at 600°C.

Infiltration of alternative materials such as alkali-earth metal compounds $BaCO_3$,[16] $SrCO_3$,[17] CaO,[18] and MgO[19] is another strategy to improve the cathode performance that has proved effective for O-SOFCs; For example, $BaCO_3$ infiltration decreased the polarization resistance of an LSCF electrode from 0.4 Ω cm^2 to 0.16 Ω cm^2 at 700°C.[16] When $SrCO_3$ nanoparticles were used as the synergetic catalyst, the cell performance was increased by a factor of 1.9.[17]

We report herein the catalytic activity of $BaCO_3$ nanoparticles on an LSCF cathode formed by thermal decomposition of barium acetate, $Ba(Ac)_2$. Electrochemical impedance spectroscopy (EIS) was applied to investigate the interfacial polarization resistance of the LSCF electrode with $BaCe_{0.7}Zr_{0.1}Y_{0.1}Yb_{0.1}O_{3-\delta}$ (BCZYYb) electrolyte, and an extended long-term test was carried out to confirm the chemical stability of the $BaCO_3$ nanoparticles on the LSCF cathode. The results show that excellent single-cell performance was achieved for the optimized $BaCO_3$ loading.

EXPERIMENTAL PROCEDURES

Powder Preparation

LSCF powder was synthesized using an ethylenediaminetetraacetic acid (EDTA)–citric acid combustion method.[20] Stoichiometric amounts of precursors $La(NO_3)_3$, $Sr(NO_3)_2$, $Co(NO_3)_3$, and $Fe(NO_3)_3$ (99.5%, Sinopharm Chemical Reagent Co.) were dissolved in distilled water, then citric acid and EDTA were added to the solution at metal/citric acid/EDTA ratio of 1:1:1, as the chelating agent to assist the combustion process. The precursor solution was heated on a hot plate until self-combustion occurred. The resulting powder was calcinated at 800°C for 2 h to remove organic residue from the ash and form a perovskite structure.

BCZYYb electrolyte precursor powder and 40 wt.% BCZYYb + 60 wt.% NiO anode precursor powder were prepared by a simple mixing and drying process. For the electrolyte precursor powder, stoichiometric amounts of $BaCO_3$, CeO_2, ZrO_2, Y_2O_3, and Yb_2O_3 with addition of 1.0 wt.% NiO as sintering aid were mixed together in isopropanol with 3-mm yttria-stabilized zirconia (YSZ) beads for 48 h, followed by drying at 90°C for 24 h. For the anode precursor powder, proper amounts of $BaCO_3$, CeO_2, ZrO_2,Y_2O_3, and Yb_2O_3 with 20 wt.% starch as pore former were blended using the same ball-milling and drying procedures as used for the electrolyte precursor.

Cell Fabrication

To form symmetrical LSCF cells, dense electrolyte pellets were synthesized by a cost-effective solid-state sintering method.[21] The electrolyte precursor powder was dry-pressed under 250 MPa for 1 min in a circular carbon-aided steel die with diameter of 15 mm to obtain green electrolyte pellets. The green pellet was sintered at 1450°C for 12 h to obtain a dense electrolyte, followed by polishing. LSCF slurry was prepared by mixing LSCF powder with organic binder and dispersant. The as-prepared slurry was printed on both sides of the BCZYYb pellets. After drying by infrared lamp, the symmetrical cell was obtained by heating at 1050°C for 2 h.

For the single cells, anode precursor powder was dry-pressed under 160 MPa for 1 min in a circular carbon-aided steel die with diameter of 19 mm to produce green anode pellets. Electrolyte precursor powder was mixed with binder and dispersant to form electrolyte slurry that was deposited on each side of the green anode pellets by screen-printing, followed by cosintering at 1450°C for 12 h. As-prepared LSCF slurry was printed on the electrolyte side and sintered at 1050°C for 2 h to obtain the full cell.

A stoichiometric amount of barium acetate, $Ba(Ac)_2$ (99%, Alfa Aesar Co. Ltd.) was dissolved in water to form 0.3 mol L^{-1} solution. Different amounts of $Ba(Ac)_2$ were infiltrated into the LSCF electrode and fired at 800°C in air for 1 h to form $BaCO_3$ nanoparticle catalyst. By controlling the volume of $Ba(Ac)_2$ solution, the loading on the cathode was varied from 3.17 wt.% to 12.02 wt.%.

Microstructure of Cathodes

The microstructure of the $BaCO_3$-infiltrated cathode and the morphology of the single cell were studied by scanning electron microscopy (SEM).

Electrochemical Measurements

The electrochemical performance of the cathode was tested using symmetrical fuel cells from 550°C to 700°C. Silver paste was printed onto both surfaces of the electrode, working as current collectors. Electrochemical impedance spectra were obtained using an electrochemical workstation (Solartron®, SI 1287 + 1260) at alternating current (AC) amplitude of 10 mV in the frequency range from 1 MHz to 10 mHz. AC impedance plots were fit using ZView software according to the equivalent circuit. The performance of single cells was tested with the cathode exposed to dry air and the anode to humified (3% H_2O) hydrogen. Single cells were sealed in an aluminum tube by ceramic bond, and silver wires were used as voltage and current leads.

RESULTS AND DISCUSSION

Formation of $BaCO_3$ Nanoparticles on the LSCF Surface

Figure 1a shows SEM micrographs of the LSCF electrode on dense BCZYYb electrolyte. The representative porous electrode exhibited good interfacial connection with the electrolyte and revealed a fine microstructure with grain size of nearly 0.2 μm. No apparent pores were observed in the dense electrolyte. Figure 1b and c shows the distribution of $BaCO_3$ nanoparticles on the LSCF electrode. Nanoscale $BaCO_3$ particles were uniformly deposited on the LSCF grain surface with particle size of approximately 20–30 nm (Fig. 1c). The areal density of nanoparticles for this loading was estimated to be approximately 5 particles/cm^2. No aggregation or coarsening of nanoparticles was observed to occur during fabrication of the cell.

Representative EIS Results for Different Loadings of $BaCO_3$ at Different Temperatures

The catalytic effect was demonstrated using the composite electrodes infiltrated with different amounts of $BaCO_3$ particles. Symmetrical cells with varying amounts of $BaCO_3$ loading demonstrated reduced polarization resistance over the entire testing temperature range, from 700°C to 600°C, as compared with the bare LSCF electrode as shown in Fig. 2. This decrease of the polarization resistance can principally be attributed to the synergetic catalytic activity of the $BaCO_3$ catalyst. However, due to the rough electrolyte surface (Fig. 1a), some of this variability in the polarization resistance could also be due to inherent thickness variations of the electrolyte. Note that both high and low loadings of $BaCO_3$ resulted in decreased polarization resistance. The lowest polarization resistance was achieved with 8.74 wt.% $BaCO_3$ at different temperatures; For example, the polarization resistance decreased by nearly 75% from 1.123 Ω cm^2 to 0.293 Ω cm^2 at 700°C, demonstrating the catalytic activity for the ORR in the LSCF electrode. Increasing the coverage and connectivity of the infiltrated nanoparticles caused a gradual reduction in the polarization resistance for the electrodes with single-digit weight percentages of $BaCO_3$. The decrease of the arc in the mid-frequency range (or the second arc from the high-frequency intercept with the real

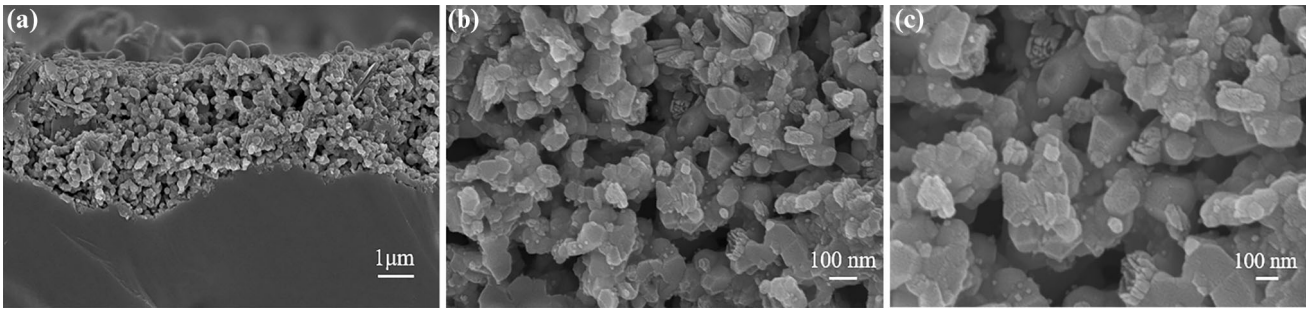

Fig. 1. Microstructure of (a) LSCF electrode and BCZYYb electrolyte and (b, c) 8.74 wt.% $BaCO_3$ nanoparticles on LSCF electrode.

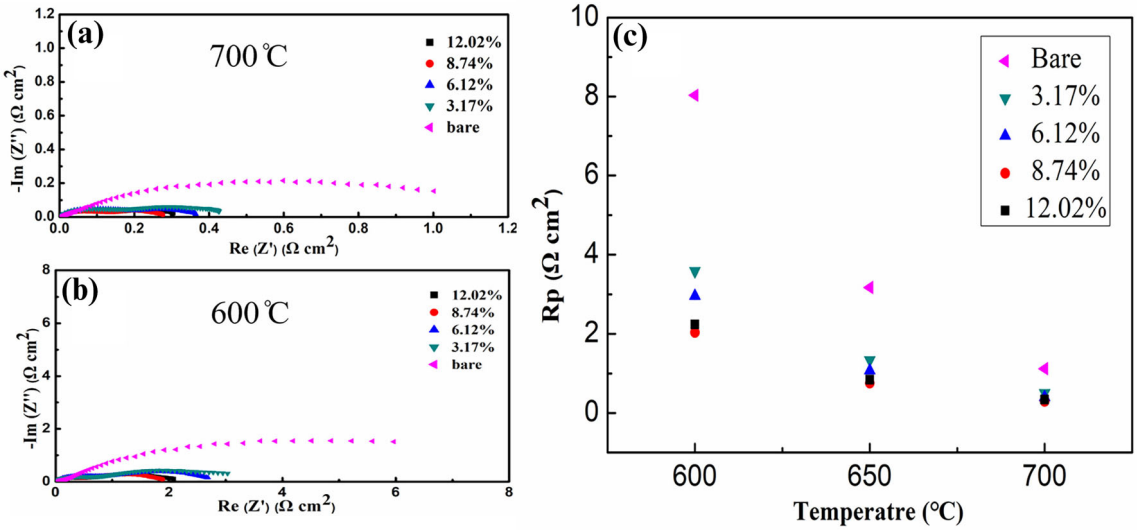

Fig. 2. Representative EIS results of LSCF symmetrical cells with different $BaCO_3$ loadings at (a) 700 °C and (b) 600 °C; (c) Comparison of polarization resistance of symmetrical cells with different $BaCO_3$ loadings from 700 °C to 600 °C.

axis) indicates that the surface reaction process in the electrodes was improved by the infiltration. Further addition of $BaCO_3$ may affect the diffusion of gases to active sites. The tails of the impedance spectra in the low frequency range, observed for the cathode with 12.02 wt.% $BaCO_3$, may indicate the occurrence of concentration polarization due to excess loading.

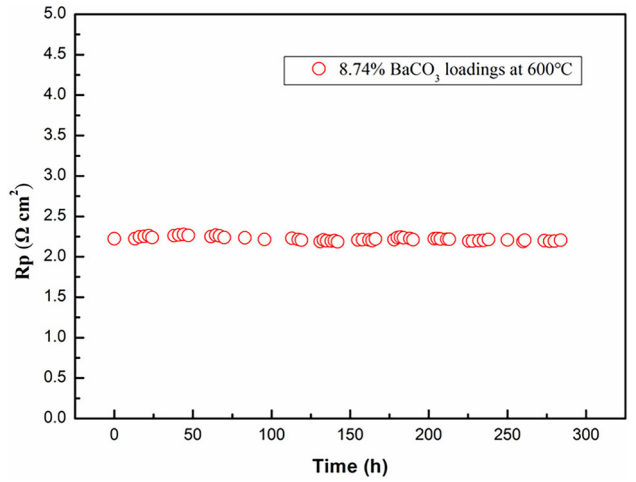

Fig. 3. Polarization resistance of LSCF electrode with 8.74 wt.% $BaCO_3$ after extended testing at 600 °C for nearly 300 h.

Long-Term Stability of Optimized Symmetrical Cell

Figure 3 shows the long-term stability of the optimized symmetrical fuel cells at 600°C, indicating negligible degradation over the duration examined in this work. The interfacial polarization resistance remained stable over nearly 300 h of testing, varying from 2.22 Ω cm^2 to 2.20 Ω cm^2. This indicates that the $BaCO_3$ material is stable on the LSCF backbone, with limited reaction between the $BaCO_3$ particles and LSCF electrode, and limited agglomeration or coarsening of the $BaCO_3$ nanoparticles.

This result is further confirmed by the microstructure of the $BaCO_3$ nanoparticles before and after the long-term test (Fig. 4). The size of the nanoscale $BaCO_3$ was nearly the same before and after the long-term stability test. This indicates that the $BaCO_3$ nanoparticles maintained their shape and crystalline structure after 300 h at 600°C, providing a potential solution for long-term proton conducting fuel cell applications.

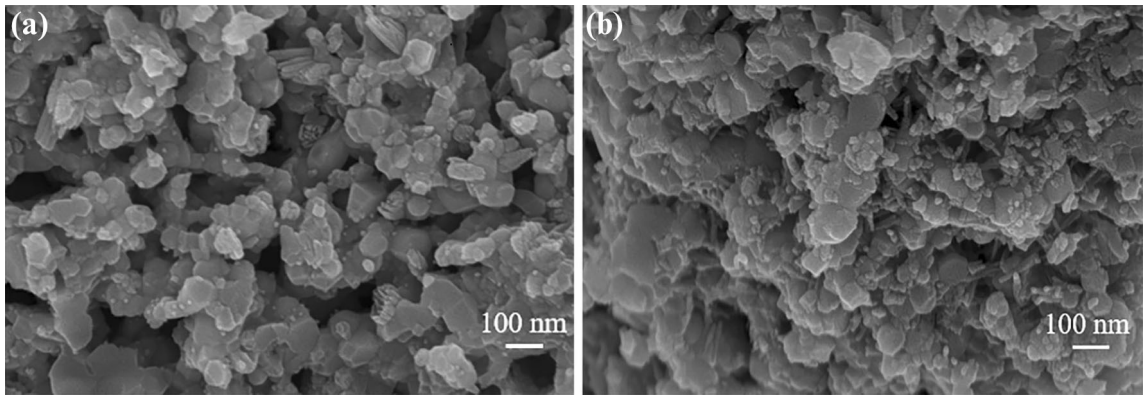

Fig. 4. Microstructure of $BaCO_3$ nanoparticles in LSCF electrode (a) before and (b) after long-term test.

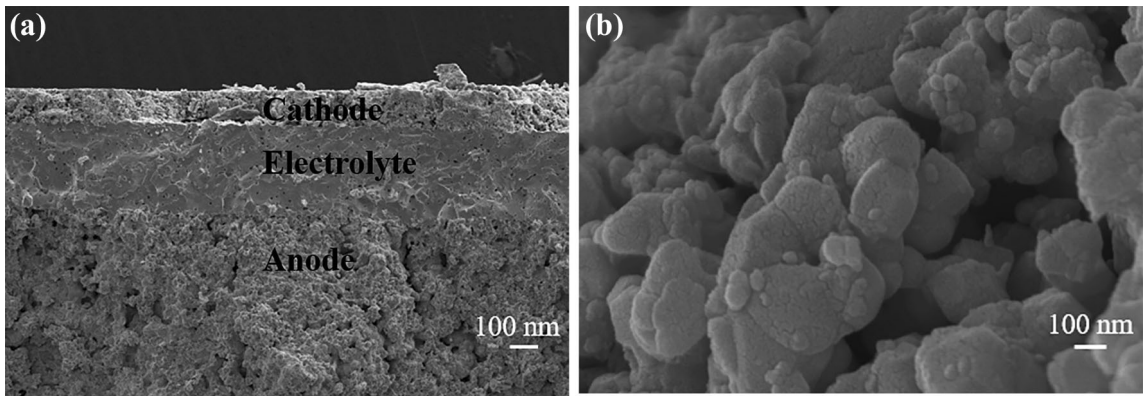

Fig. 5. Microstructure of (a) the single cell and (b) LSCF electrode with $BaCO_3$ nanoparticles.

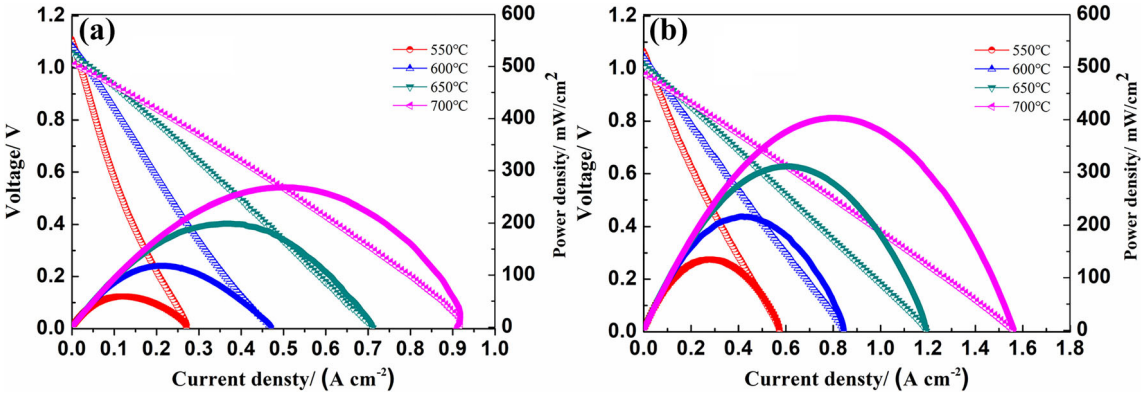

Fig. 6. Voltage and power density versus current density for (a) bare LSCF electrode and (b) composite electrode with 8.7 wt.% $BaCO_3$ nanoparticles.

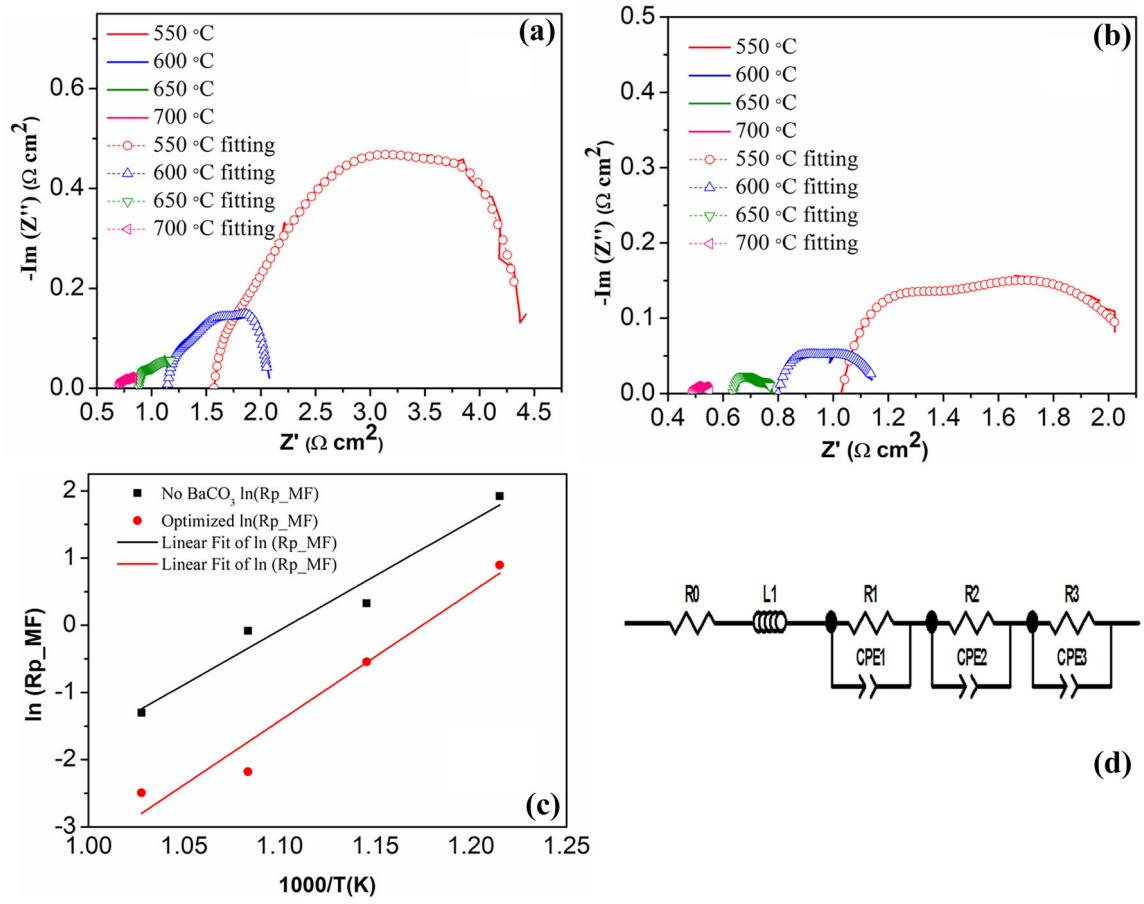

Fig. 7. Electrochemical impedance spectra measured from 700 °C to 550 °C for (a) single cell with bare LSCF electrode and (b) single cell with optimized LSCF electrode; (c) Arrhenius plot of polarization resistance from cathode for bare single cell and optimized single cell; (d) equivalent circuit for fitting the impedance spectra.

Single-Cell Performance

An LSCF electrode with the optimized $BaCO_3$ loading (8.74 wt.%) was used as a cathode for single-cell testing. The trilayer-structured membrane of the single cell is displayed in Fig. 5. The electrolyte was nearly 60 μm thick, being densely structured to ensure a high open voltage for the single cell. It was noted that the $BaCO_3$ nanoparticles were distributed on the LSCF backbone with approximately the same size as observed in the symmetrical cell studies. Open pores were observed in the supporting substrate, which

should favor gas diffusion during the electrode reaction processes.

Figure 6 shows typical cell voltage (V) and power density (P) results as a function of the current density (J). The maximum power density of the LSCF electrode with no $BaCO_3$ loading was 268 mW cm^{-2}, 199 mW cm^{-2}, 118 mW cm^{-2}, and 58 mW cm^{-2} at 700°C, 650°C, 600°C, and 550°C, respectively. These results are comparable to those obtained in Hanifi's[22] study, using 10 μm BCZYYb as the electrolyte and LSCF as the cathode (166 mW cm^{-2} and 218 mW cm^{-2} at 600°C, 650°C, and 700°C, respectively). The maximum power density increased by nearly 50% with addition of the optimized $BaCO_3$ loading (8.74 wt.%), reaching 404 mW cm^{-2}, 312 mW cm^{-2}, 217 mW cm^{-2}, and 135 mW cm^{-2} at 700°C, 650°C, 600°C, and 550°C, respectively. This increased maximum power density is due to the catalytic effect of the deposited $BaCO_3$ nanoscale particles on the LSCF backbone.

Figure 7a and b shows the electrochemical impedance spectra for the single cells measured at between 550°C and 700°C. The equivalent circuit used for data fitting is shown in Fig. 7d. R0 is the serial resistance due to the electrolyte, electrodes, and connection wires; L1 is the inductance; R1-CPE1, R2-CPE2, and R3-CPE3 are the electrode resistive elements corresponding to the high-, mid-, and low-frequency arcs, respectively. It is evident that the polarization resistance was significantly reduced for the optimized LSCF cathode. According to high-resolution impedance study for anode-supported cells, the arc in the mid-frequency range (i.e., from 3 Hz to 300 Hz) is associated with cathode activation polarization.[23] The equivalent circuit model analysis confirmed that the reduction in the total polarization resistance for the single cell with the optimized cathode originated from cathode activation, as presented in Fig. 7c for the mid-frequency resistance (R2), suggesting that the $BaCO_3$ nanoparticles effectively improved the ORR activity of the bare LSCF cathode.

CONCLUSION

$BaCO_3$ nanoparticles were deposited on LSCF electrodes by a wet-chemistry infiltration method for enhanced performance of proton ceramic SOFCs. Catalytic effects were demonstrated when using an LSCF electrode with varying amounts of barium carbonate loading. The polarization resistance of the electrode decreased by nearly 75% from 1.123 Ω cm^2 to 0.293 Ω cm^2 at 700°C, mainly due to the low-frequency polarization resistance which corresponds to the surface reaction process. The optimized symmetrical cell exhibited good chemical stability and physical stability with limited coarsening observed after an extended test for 300 h. The maximum power density increased by 50%, from 268 mW cm^{-2} to 404 mW cm^{-2} at 700°C. $BaCO_3$ demonstrated promising performance enhancement of LSCF electrodes in H-SOFCs and warrants further testing in additional cathode systems.

ACKNOWLEDGEMENTS

K.S.B. was supported in part by an appointment to the National Energy Technology Laboratory Research Participation Program, sponsored by the U.S. Department of Energy and administered by the Oak Ridge Institute for Science and Education. We also gratefully acknowledge financial support from the Department of Energy, Nuclear Energy Research Program (DOE-NEUP) Project: 17-12798: Nanostructured Ceramic Membranes for Enhanced Tritium Management.

REFERENCES

1. N.Q. Minh, *J. Am. Ceram. Soc.* 76, 563 (1993).
2. Z. Zhan, *Science* 308, 844 (2005).
3. S. Park, J.M. Vohs, and R.J. Gorte, *Nature* 404, 265 (2000).
4. S.M. Haile, *Acta Mater.* 51, 5981 (2003).
5. E. Fabbri, L. Bi, D. Pergolesi, and E. Traversa, *Adv. Mater.* 24, 195 (2012).
6. J. An, Y.-B. Kim, J. Park, T.M. Gür, and F.B. Prinz, *Nano Lett.* 13, 4551 (2013).
7. Z. Shao and S.M. Haile, *Nature* 431, 170 (2004).
8. J. Gao, X. Meng, T. Luo, H. Wu, and Z. Zhan, *Int. J. Hydrog. Energy* 42, 18499 (2017).
9. S.P. Jiang, *Int. J. Hydrog. Energy* 37, 449 (2012).
10. X. Liu, H. Wu, Z. He, J. Gao, X. Meng, T. Luo, C. Chen, and Z. Zhan, *Int. J. Hydrog. Energy* 42, 18410 (2017).
11. S. Jiang, *Solid State Ionics* 146, 1 (2002).
12. E. Perry, Murray. *Solid State Ion.* 148, 27 (2002).
13. L. Lei, Z. Tao, T. Hong, X. Wang, and F. Chen, *J. Power Sources* 389, 1 (2018).
14. G. Li, B. He, Y. Ling, J. Xu, and L. Zhao, *Int. J. Hydrog. Energy* 40, 13576 (2015).
15. B. He, L. Zhang, Y. Zhang, D. Ding, J. Xu, Y. Ling, and L. Zhao, *J. Power Sources* 287, 170 (2015).
16. T. Hong, K.S. Brinkman, and C. Xia, *ChemElectroChem* 3, 805 (2016).
17. M. Li, Z. Sun, W. Yang, T. Hong, Z. Zhu, Y. Zhang, X. Wu, and C. Xia, *Phys. Chem. Chem. Phys.* 19, 503 (2017).
18. L. Zhang, T. Hong, Y. Li, and C. Xia, *Int. J. Hydrog. Energy* 42, 17242 (2017).
19. Y. Yang, M. Li, Y. Ren, Y. Li, and C. Xia, *Int. J. Hydrog. Energy* 43, 3797 (2018).
20. J. Martynczuk, M. Arnold, H. Wang, J. Caro, and A. Feldhoff, *Adv. Mater.* 19, 2134 (2007).
21. C. Duan, J. Tong, M. Shang, S. Nikodemski, M. Sanders, S. Ricote, A. Almansoori, and R.O. Hayre, *Science* 349, 1321 (2015).
22. A.R. Hanifi, N.K. Sandhu, T.H. Etsell, and P. Sarkar, *J. Am. Ceram. Soc.* 100, 4983 (2017).
23. A. Leonide, V. Sonn, A. Weber, and E. Ivers-Tiffée, *J. Electrochem. Soc.* 155, B36 (2008).